Boosting the Thermoelectric Performance of Zinc Blende-like Cu_2SnSe_3 through Phase Structure and Band Structure Regulations

Meng Wang,[1,#] Mingkai He,[2,#] Lujun Zhu,[3,*] Baopeng Ma,[1] Fudong Zhang,[1] Pengfei Liang,[3] Xiaolian Chao,[1] Zupei Yang[1,*] Di Wu[1,*] and Jiaqing He[4]

[1] Key Laboratory for Macromolecular Science of Shaanxi Province, School of Materials Science and Engineering, Shaanxi Normal University, Xi'an 710119, China
[2] Department of Physics, The Chinese University of Hong Kong, Hong Kong 999077, China
[3] School of Physics and Information Technology, Shaanxi Normal University, Xi'an 710119, China
[4] Department of Physics, South University of Science and Technology of China, Shenzhen 518055, China
[#] These authors contributed equally to this work
* Correspondence shall be addressed to:
E-mail: zhulujun@snnu.edu.cn, yangzp@snnu.edu.cn, wud@snnu.edu.cn

EXPERIMENTAL SECTION

Sample preparations

$Cu_2(Sn_{1-2x}In_xSb_x)Se_3$ (x = 0, 0.025, 0.05, 0.075 and 0.01) and $Cu_2(Sn_{0.9-y}In_{0.05}Sb_{0.05}Ti_y)Se_3$ (y = 0, 0.025, 0.05 and 0.075) samples were prepared *via* a solid-melt followed by spark plasma sintering method. Cu (99.99%), Sn (99.99%), Se (99.999%), In (99.99%), Sb (99.999%), Ti (99.99%) with nominal compositions were mixed and sealed in quartz tubes under vacuum (< 10^{-4} Pa). Sealed tubes were heated in a muffle furnace at a rate of 4.8 K min^{-1} to 1173 K, and held at this temperature for 12 h, then furnace cooled to room temperature. Obtained ingots were grinded in an agate mortar into fine powders, and then loaded in graphite dies to be sintered into coins of dimension Φ15.6 mm *via* the spark plasma sintering system (SPS, LABOX-212) at 773 K for 5 min with the pressure of 50 MPa under vacuum.

Phase structure and microstructure characterizations

The phase structures of obtained samples were characterized by a commercial X-ray diffraction (XRD, Rigaku, MiniFlex 600) apparatus, using Cu-Kα radiation; the 2θ

range was set between 10° and 80° with an increment interval of 0.02°. The Rietveld refinement quantitative phase analyses were conducted using a GSAS software[1].

Before being characterized under SEM, samples were sealed in vacuum in quartz tubes, and thermally etched at 673K, for 30 minutes. The surfaces of obtained samples were then observed under a tungsten filament scanning electron microscope (SEM, Hitachi, SU3500) at a 5 kV voltage.

Specimens for high-resolution STEM observations were prepared by mechanical polishing, dimpling, and argon ion milling, where a final cleaning was performed using 0.5 keV Ar^+ ions with a liquid nitrogen stage. Spherical aberration-corrected (Cs-corrected) high-angle annular dark-field scanning transmission electron microscopy (HAADF-STEM) was performed using a FEI Titan Themis 60-300 kV microscope equipped with a Super-X detector and operating at 300 kV.

Physical property characterizations

All the samples were cut into bars with size of 3 × 3 × 12 mm for electrical conductivity (σ) and Seebeck coefficient (S) measurements in a commercial Ulvac Riko ZEM-3 (Japan) instrument. The uncertainties of electrical conductivity (σ) and Seebeck coefficient (S) measurements are within 5 %. Charge carrier concentration and mobility were obtained *via* Hall measurements conducted in a commercial Lakeshore 8400 (US) apparatus.

For thermal conductivity, the total thermal conductivity (κ_{tot}) can be derived by $\kappa_{tot} = D\ \rho\ C_p$; wherein, thermal diffusivity D was determined by the laser flash diffusivity method with a Netzsch LFA-467 instrument (Germany), the specific heat (C_p) was the theoretical Dulong-Petit limit $3R/M$ where M is the molar mass of each composition, mass density (ρ) was measured using the Archimedes' method. The uncertainty of thermal diffusivity measurement is ~ 8 %.

Combining the uncertainties of all measurements, the uncertainty of calculated figure of merit ZT is about ~ 13 %. Electrical thermal conductivity was calculated by the Wiedemann-Franz law[2]:

$$\kappa_e = L\sigma T \qquad \text{* MERGEFORMAT (1)}$$

Where L is the Lorenz number calculated by the formula[2]:

$$L = 1.5 + \exp\left(-|S|/116\right) \qquad \text{* MERGEFORMAT (2)}$$

And the lattice thermal conductivity can then be derived as:

$$\kappa_L = \kappa_{tot} - \kappa_e \qquad \text{* MERGEFORMAT (3)}$$

Density Function Theory calculations

The total energy, electronic band structure, and density of states in this study were calculated by the projector augmented wave (PAW) method, as implemented in the Vienna Ab initio Simulation Package (VASP).[3, 4] The exchange and correlation potentials for lattice structure optimization and total energy comparison are evaluated by using Perdew-Burke-Ernzerhof (PBE) functional of the generalized gradient approximation (GGA).[5] Since the underestimated band gaps and the band structures nearing the valence band maximum (VBM) obtained using PBE functional were highly unreliable, the hybrid functional (HSE06)[6, 7] was selected as the exchange-correlation functional to perform the calculations of band structure and density of states. The lattice parameters of cubic and monoclinic CTSe used in the calculations come from the Rietveld refinement of powder X-ray diffraction data. The calculations were conducted in a primitive cell for monoclinic (12 atoms) and an unit cell (96 atoms) for cubic phase CTSe. A 2×2×1 monoclinic supercell (48 atoms) was constructed with two Sn atoms being substituted by a In atom and a Sb atom to examine the In, Sb co-doping effect on monoclinic CTSe lattice. A Γ-centered Monkhorst-Pack ***k***-point mesh with density of $2\pi \times 0.03$ Å^{-1} was applied for Brillouin zone sampling,[8] and a plan-wave cutoff energy of 400 eV, an energy convergence criterion of 10^{-6} eV were employed for all calculations.

Calculated total energies and formation energies for monoclinic and cubic structures are list as follows:

$$E_F = E_{tot} - \sum_i \eta_i \mu_i \qquad \text{* MERGEFORMAT (4)}$$

E_{tot} (Monoclinic CTSe) = -23.24525 eV

E_{tot} (Cubic CTSe) = -23.44319 eV

μ_{Se} = -3.50554 eV

μ_{Cu} = -3.72233 eV

μ_{Sn} = -3.84626 eV

E_F (Monoclinic CTSe) = -1.6356 eV

E_F (Cubic CTSe) = -1.4377 eV

SUPPLEMENTAL FIGURES

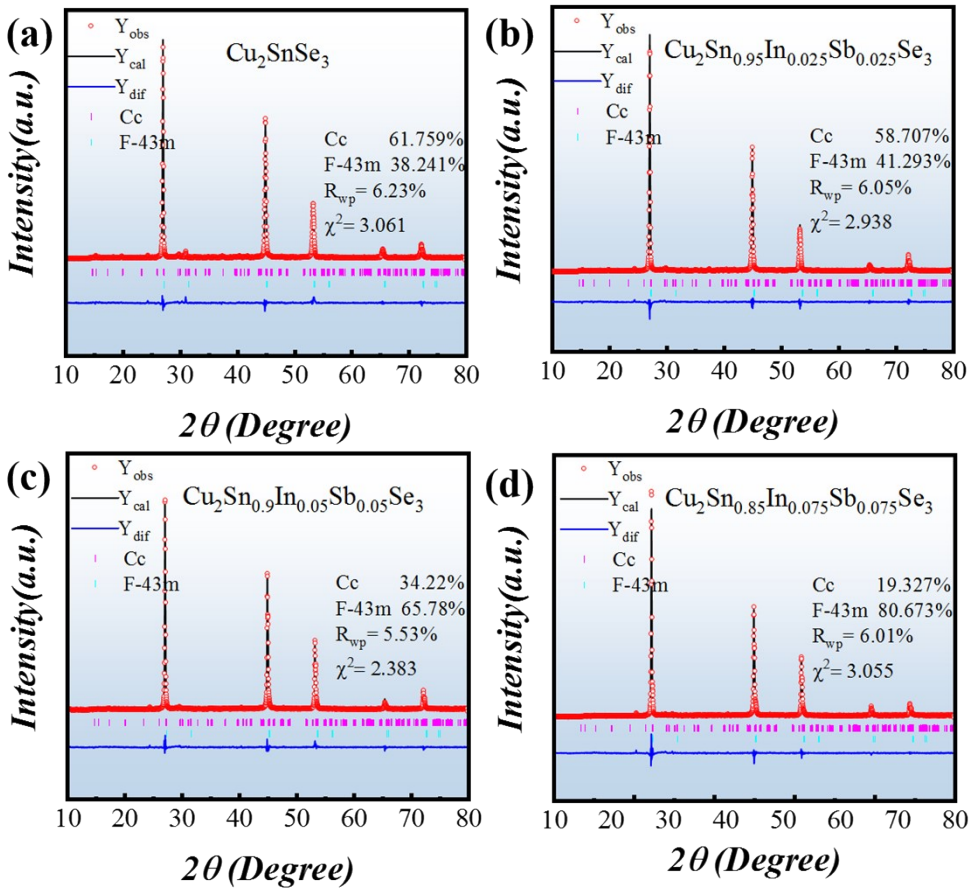

Figure S1. Rietveld refinement quantitative phase analyses along with R_{wp} and χ^2 values for individual samples of (a) Cu_2SnSe_3; (b) $Cu_2Sn_{0.95}In_{0.025}Sb_{0.025}Se_3$; (c) $Cu_2Sn_{0.9}In_{0.05}Sb_{0.05}Se_3$; (d) $Cu_2Sn_{0.85}In_{0.075}Sb_{0.075}Se_3$.

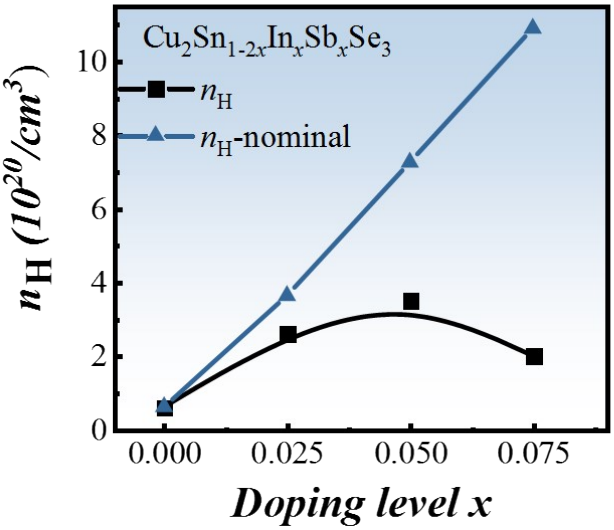

Figure S2. The scheme illustrating measured Hall carrier concentration VS nominal carrier concentration in In/Sb co-doping system.

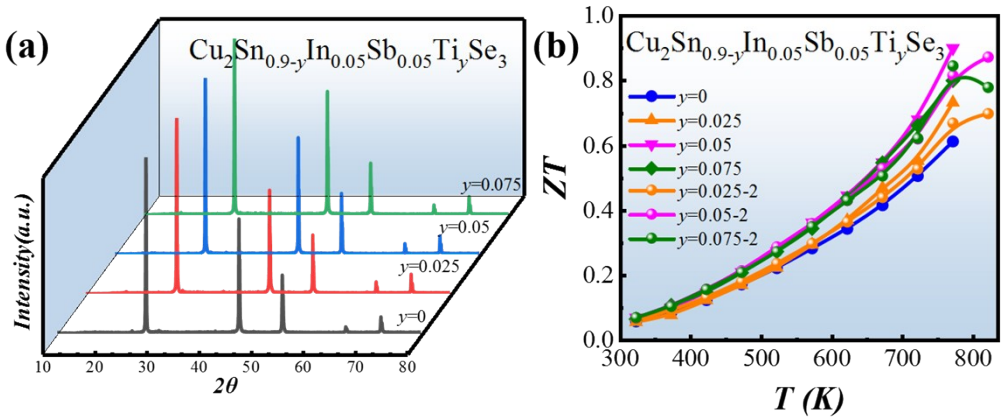

Figure S3. (a) Powder XRD patterns of $Cu_2Sn_{0.9-y}In_{0.05}Sb_{0.05}Ti_ySe_3$ (y = 0, 0.025, 0.05 and 0.075) samples; (b) the repeatability of the Ti doped $Cu_2Sn_{0.9-y}In_{0.05}Sb_{0.05}Ti_ySe_3$ samples (y = 0, 0.025, 0.05 and 0.075) were obtained by increasing the test temperature to 823K.

Table S1. Parameters used for Debye-Callaway model

PARAMETERS	DESCRIPTION	VALUES
θ_D[9]	Debye temperature for Cu_2SnSe_3, $Cu_2Sn_{0.85}Sb_{0.075}In_{0.075}Se_3$ and $Cu_2Sn_{0.85}Sb_{0.05}In_{0.05}Ti_{0.05}Se_3$	231K;231K;230K
V[9]	Average atomic volume of Cu_2SnSe_3	$2.292*10^{-29}$,
M	Average atomic mass for Cu_2SnSe_3,$Cu_2Sn_{0.85}Sb_{0.075}In_{0.075}Se_3$ and $Cu_2Sn_{0.85}Sb_{0.05}In_{0.05}Ti_{0.05}Se_3$	1.3363e-25kg;1.3362e-25kg;1.3362e-25kg
v_i	Average sound speed	$v_{(i)}$=2200-0.2*($T_{(i)}$-323);%
β	Ratio of N- to U-processes	1.3(fitted)

References:

1 B. H. Toby, *J. Appl. Crystallogr.*, 2001, **34**, 210-213.

2 A. F. May, E. S. Toberer, A. Saramat and G. J. Snyder, *Phys. Rev. B*, 2009, **80**, 125205.

3 G. Kresse and J. Furthmüller, *Phys. Rev. B*, 1996, **54**, 11169-11186.

4 G. Kresse and D. Joubert, *Phys. Rev. B*, 1999, **59**, 1758-1775.

5 J. P. Perdew, K. Burke and M. Ernzerhof, *Phys. Rev. Lett.*, 1996, **77**, 3865-3 868.

6 J. Heyd, G. E. Scuseria and M. Ernzerhof, *J. Chem. Phys.*, 2003, **118**, 8207-8215.

7 A. V. Krukau, O. A. Vydrov, A. F. Izmaylov and G. E. Scuseria, *J. Chem. Phys.*, 2006, **125**, 224106.

8 H. J. Monkhorst and J. D. Pack, *Phys. Rev. B*, 1976, **13**, 5188-5192.

9 H. Ming, G. Zhu, C. Zhu, X. Qin, T. Chen, J. Zhang, D. Li, H. Xin and B. Jabar, *ACS Nano*, 2021, **15**, 10532-10541.